

# Development of heavyweight concrete incorporating steel slag as aggregate for potential application of wave-dissipating blocks in Vietnam

Duong Trung Quoc, Tran Thanh Nhan\*, Tran Thi Ngoc Quynh, Nguyen Thi Le Huyen,  
Do Quang Thien

University of Sciences, Hue University, Hue, Vietnam

\* Correspondence to Tran Thanh Nhan <ttnhan@hueuni.edu.vn>

(Received: 24 April 2026; Revised: 07 May 2026; Accepted: 09 May 2026)

**Abstract.** In 2024, Vietnam ranked as the 11th largest steel producer worldwide, with an annual crude steel output of approximately 22 million tonnes, generating a substantial amount of steel slag (SS). As most major steel plants in Vietnam employ Basic Oxygen Furnace (BOF) technology, BOF slag represents the dominant type of SS produced. This study proposes and evaluates the use of mixed BOF and cast SS, based on actual production proportions at the Formosa steel plant, as coarse aggregates for heavyweight concrete (SS concretes) under Vietnamese conditions. Four qualified SS types were combined and applied in concrete mixtures across three grading scenarios. The results show that SS concretes exhibit more consistent compressive strength development and more significant strain at failure than conventional concretes made with natural aggregates. The 28-day compressive strength of the SS concretes reached 113.6–117.8% of the target strength for M400 concrete. Owing to the higher density of the SS aggregates (1.23–1.42 times that of natural aggregates), the resulting concretes achieved densities 1.13–1.16 times greater than conventional mixes, with average values ranging from 2.64 to 2.73 t/m<sup>3</sup>, meeting the requirements for heavyweight concrete. These findings indicate that SS concrete has potential for applications such as wave-dissipating blocks; however, further hydraulic investigations are required to confirm this performance.

**Keywords:** coarse aggregate, compressive strength, heavyweight concrete, steel slag, wave-dissipating blocks

## 1 Introduction

Steel slag (SS), a by-product of the steel-making process, accounts for approximately 10–15% by mass of finished steel; in Vietnam, this share reaches roughly 15%. Specifically, global SS production was projected to range from 190 to 290 million tons (Mt.) [1]. Consequently, the recycling of SS is a heavy duty of the steel industry and has become a cumulatively attractive topic among researchers worldwide. Due to its substantial volumes and favorable properties, SS is mainly used as a substitute for natural materials in the construction sector [2–6]. Steel slag exhibits

inherent heterogeneity and perceived latent risks because its composition and characteristics are driven by the input materials and manufacturing processes of the steel plant. On the other hand, the demand for the use of SS in the construction field is a very large, and the construction works over a long time under various natural environments and conditions. Therefore, the utilisation rate of SS, particularly for large-scale application, depends primarily on the level of research development and the refinement of specification and standard systems that are tailored to the intrinsic characteristics of SS, as well as to the specific application domains within each nation

[2–4, 6]. In order to regulate the management and promote the utilisation of SS, several countries established national and regional slag associations decades ago, such as the National Slag Association (established 107 years ago), the Nippon Slag Association (47 years), the Australasian (iron & steel) Slag Association (35 years), and the European Slag Association (32 years). Consequently, as of 2018, the utilisation rate of SS in Europe has reached 72.3%, while in Japan and the United States, this proportion exceeded 85%. In contrast, in China and India – the world’s largest steel producers – the utilisation rate remained significantly lower, at approximately 30 and 17%, respectively [5–7].

Steel slag exhibits superior physico-mechanical properties compared with conventional natural aggregates (e.g., crushed basalt or limestone), including high hardness, strong abrasion resistance, pronounced angularity, rough surface texture, enhanced crushing resistance, and greater shear strength [6, 8–12]. These characteristics make SS a promising alternative material for construction applications. Previous studies have reported its use as a filler or cementitious material in subgrade stabilisation, as aggregate in asphalt pavements and base courses, as a functional material for anti-skid and noise-reducing surfaces, and as aggregate in concrete [4, 6, 9, 11, 13–16].

However, several technical challenges limit its widespread application. First, the rough surface texture and high crushing resistance of SS require higher compaction energy and complicate construction control [17]. Its porous structure and surface voids increase water and binder absorption, especially when used as fine aggregate [18–20]. In addition, the higher specific gravity of SS (3.2–3.7) than that of natural aggregates (2.6–2.8) leads to increased transportation costs and a greater risk of

segregation during mixing [21, 22]. Environmental concerns also arise because of its high CaO content, which results in strong alkalinity and potential leaching of heavy metals under weathering conditions, posing risks to soil and groundwater if improperly managed [4–6]. Furthermore, volumetric instability caused by free lime (f-CaO) and free magnesia (f-MgO) remains a critical concern when SS is used in construction [4, 9].

Despite these limitations, most existing studies focus on single-type SS or controlled laboratory conditions, while limited attention has been given to the combined use of multiple SS types, reflecting actual industrial production proportions. In Vietnam, where BOF slag is a dominant by-product, there is a lack of systematic investigation into the use of mixed SS as coarse aggregate for concrete, particularly in relation to grading design and its influence on mechanical performance and density characteristics.

Therefore, this study aims to evaluate the feasibility of using mixed SS, derived from actual production at a major steel plant, as coarse aggregate for heavyweight concrete. The research specifically focuses on the effects of different grading scenarios on compressive strength development, deformation behaviour, and density, thereby providing a practical basis for the utilisation of SS in concrete under Vietnamese conditions.

## **2 Current status and valorisation orientation of SS in Vietnam**

### **2.1 Steel slag generation and utilisation**

Currently, over 27 major steel plants operate in Vietnam, most of which are located in coastal regions. Because of the absence of a governing body or a national slag association, official statistics regarding SS production remain

unavailable. In 2016, the SS production was estimated at approximately 2 Mt. [23]. By 2024, Vietnam became the 11th largest steel producer globally, with an annual crude steel production of 22 Mt. [24], a threefold increase compared with that in 2016. As of 2025, the two largest steel plants locating in the Central region, the Hoa Phat Dung Quat (HPDQ) and Ha Tinh Formosa (FHS) plants, alone have been projected to produce roughly 19.5 Mt. of steel, which is expected to generate an annual SS output of 3.03 Mt.

Early research efforts in Vietnam were primarily exploratory, focusing on the characterisation of basic compositions and fundamental properties of both ash and slag materials [25–27]. Subsequent studies have gradually transitioned toward more targeted applications, such as utilising SS as an aggregate for cement concrete [28–33], aggregate for road pavement structures [34–37], and backfilling materials [38]. However, research on SS in Vietnam remains predominantly academic-oriented and is largely confined to master’s theses and doctoral dissertations. Moreover, several studies are limited by short research durations and insufficient experimental scope; for instance, certain investigations were conducted over approximately 5.5 months with no more than three tests performed on the physico-mechanical properties and chemical composition of SS [34, 38]. As a result, these studies failed to adequately address the complex technical and environmental challenges associated with the large-scale SS utilisation.

Driven by the rapid increase in SS generation and the concurrent depletion of natural construction materials, the Vietnamese government has enacted various regulatory frameworks to promote the utilisation of industrial by-products in general, and SS in construction in particular. These initiatives have been incorporated into the national action plan

toward a green, circular, and sustainable economy. In 2017, the Ministry of Construction (MOC) issued technical guidelines for the use of iron and steel slag as building materials [39], and as of 2022, SS has been officially classified as regular solid waste [40], facilitating its management and potential reuse. Most recently, in 2024, the Ministry of Science and Technology established national standards for SS applications, including TCVN 13906:2024 for backfill materials and TCVN 13908-2:2024 for concrete aggregates [41, 42] (Table 1).

**Table 1.** Vietnamese technical guidelines, standards, and regulations related to SS

Document number	Document title	Year of issue
Decision No.430/QĐ-BXD	Guideline on iron and steel slag for use as building materials	2017
TCVN 12464:2018	Steel slag – Basic technical characteristic and test methods	2018
Circular No. 02/2022/TT-BTNMT	Circular specifying the detailed implementation of certain provisions of the Environmental Protection Law	2022
TCVN 13906:2024	Steel slag used as backfill material	2024
TCVN 13908-2:2024	Slag aggregate for concrete, Part 2: Electric arc furnace oxidising slag aggregate	2024

However, most of these standards and guidelines are largely adapted from foreign references, and TCVN 13908-2:2024 primarily addresses electric arc furnace (EAF) slag, whereas the dominant SS generated in Vietnam (including FHS and HPDQ plants) is basic oxygen furnace slag. Consequently, the majority of SS from most steel plants is currently utilised as backfill materials in accordance with TCVN 13906:2024. This prevailing practice not only poses potential

long-term environmental risks but also fails to fully exploit the functional performance and value-added potential of SS in higher-grade construction applications, particularly as alternative aggregates for concrete.

## 2.2 Application-oriented research for SS

It is indicated that Vietnam currently faces approximately 314 coastal erosion sites, and 154 of which are classified from highly to extremely dangerous levels with a total length of roughly 310 km [34]. Numerous locations have suffered from prolonged erosion; for instance, in Hoi An Ward (Da Nang City, central Vietnam), coastal erosion has caused damage to coastal protection structures since 2014 (Fig. 1a) and became emergency situation in 2025 as erosion encroached upon residential areas [44] (Fig. 1b). Consequently, coastal erosion mitigation and the protection of coastal infrastructure have emerged as urgent national priorities, as underscored by the Government's Decision No. 379/QĐ-TTg approving the National Strategy for Natural Disaster Prevention and Control toward 2030, with a vision to 2050.

A widely adopted solution for coastal protection is the use of concrete wave-dissipating blocks, among which the Tetrapod block remains the most prevalent. The minimum required mass of such blocks to resist specific wave intensities is typically determined by using the Hudson formula [45, 46]. According to this empirical relationship, the stability of the blocks is directly governed by the effective density of the concrete in seawater, accounting for buoyancy effects. Notably, an increase in concrete density ( $\rho_c$ , t/m<sup>3</sup>) by a factor of 1.13, such as transitioning from conventional concrete ( $\rho_c = 2.3$  t/m<sup>3</sup>) to heavyweight concrete ( $\rho_c = 2.6$  t/m<sup>3</sup>), results in a significant 47% reduction in the required block mass (or the block size) while maintaining

equivalent wave-dissipation performance. Alternatively, for the blocks of identical size, such an increase in the concrete density effectively doubles the wave-dissipating efficiency [46]. A reduction in the block size leads to a corresponding decrease in the total volume of concrete required, thereby lowering overall fabrication costs. Furthermore, employing smaller wave-dissipating units significantly reduces the spatial footprint of the protection system, enabling a more compact design for the coastal protection corridor. Since aggregates typically occupy 70–80% of the total concrete volume, increasing concrete density can only be effectively achieved through the use of aggregates with higher density. Specifically, to increase the concrete density from 2.3 to  $\geq 2.6$  t/m<sup>3</sup>, the aggregates should exhibit a particle density of approximately 3.0–3.2 t/m<sup>3</sup> and a loose bulk density of about 2.0–2.2 t/m<sup>3</sup>. Steel slag, with a particle density ranging from 3.2 to 3.7 t/m<sup>3</sup>, approximately 1.2–1.3 times higher than that of conventional natural aggregates such as limestone or granite, therefore represents an ideal candidate for the production of heavyweight concrete.

In this study, SS generated from the FHS plant (hereafter referred to as Formosa SS) was collected and characterised for its physico-mechanical properties to evaluate its suitability as aggregate for concrete. The SS types exhibiting appropriate properties were blended according to their generation rates and subsequently investigated for use as coarse aggregates at three particle size ranges: 5–10 mm, 5–20 mm, and 10–40 mm, and these aggregates were used to prepare concrete mix and specimen. The performance of concrete incorporating SS aggregate (hereafter referred to as SS concrete) was then evaluated and compared with that of conventional concrete with natural aggregates (crushed stone and river sand).

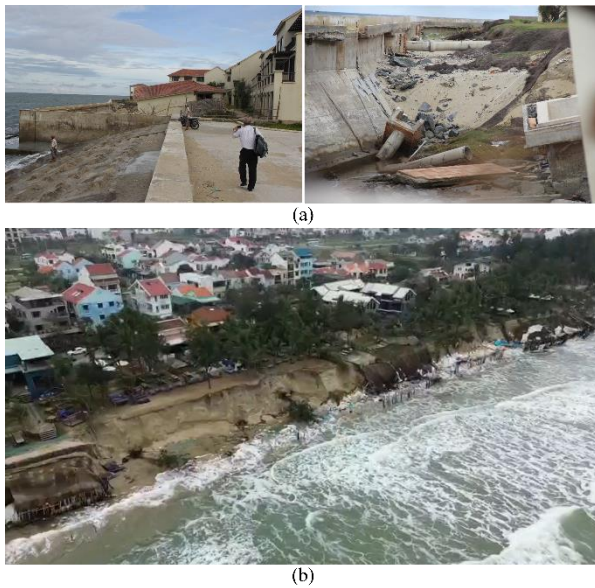


**Fig. 1.** Temporal progression of erosion-induced damage in Hoi An Ward, Da Nang City: (a) coastal erosion has caused damage to coastal protection structures since 2014, and (b) escalated into an emergency situation as erosion encroached upon residential areas from January 2025 [44]

### 3 Properties of Formosa SS

#### 3.1 Types of Formosa SS

The FHS plant utilises BOF technology for crude steel production, using metallic charge consisting of 70–80% pig iron and 20–30% scrap. This steel-making process generates three types of SS: desulfurisation slag (DeS slag), produced during the pretreatment of molten pig iron prior to BOF charging; BOF slag, formed during the primary steel-making stage for crude steel; and casting slag (CAST slag) or ladle furnace slag (LF slag), generated during the secondary refining and continuous casting processes. Upon discharge at approximately 1,500 °C, the molten slag undergoes rapid cooling, followed by standardised on-site treatments including hydration of free expansive components (particularly  $f\text{-CaO}$  and  $f\text{-MgO}$ ), crushing, sieving, and magnetic separation. The resulting BOF and CAST slags are classified into two particle size ranges: 0–10 mm (designated as BOF010 and

CAST010) and 0–40 mm (designated as BOF040 and CAST040). Consequently, the FHS plant generates five SS products: BOF010, BOF040, CAST010, CAST040, and DeS, which are stockpiled separately at a designated landfill area within the plant. To ensure material traceability and preserve original characteristics and compositions, each SS type was separately collected and stored in individual jumbo bags. Representative samples were then obtained in accordance with TCVN 7572:2006 standard series [47] for physico-mechanical characterisation, with the aim of assessing their suitability for use as concrete aggregates. Typical photos of the five Formosa SS types are illustrated in Figs. 2a–e.

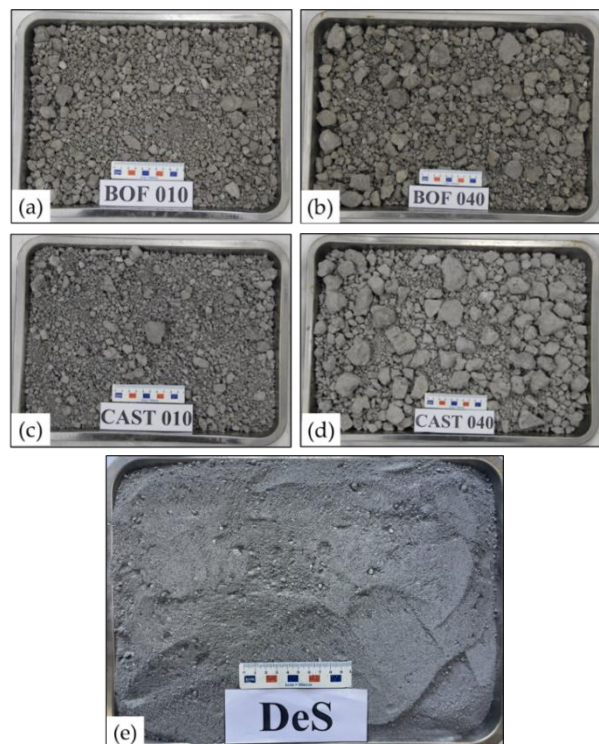


**Fig. 2.** Photos of Formosa SSs: (a) BOF040; (b) BOF010; (c) CAST040; (d) CAST010; (e) DeS

#### 3.2 Chemical compositions

In Table 2, the chemical compositions of Formosa SS are presented and compared with those of BOF and LF (CAST) slags reported in previous studies worldwide. The chemical and mineral compositions of SS are inherently complex and

vary significantly depending on steel-making processes, furnace technology, additive regimes, cooling conditions, and the type of final steel products [3, 4, 6]. The principal oxide constituents of SS are CaO, SiO<sub>2</sub>, Fe<sub>2</sub>O<sub>3</sub>, and MgO, which together typically account for approximately 80% of the total mass, forming the dominant quaternary system [2, 6]. Among these, CaO is generally the most abundant component, followed by either Fe<sub>2</sub>O<sub>3</sub> or SiO<sub>2</sub>. While BOF and EAF slags exhibit broadly similar compositions, LF slag is characterised by lower Fe<sub>2</sub>O<sub>3</sub> and higher CaO contents [3, 6].

As shown in Table 1, the chemical compositions of the Formosa SS are consistent with these reported trends, with the contents of

the four major oxides falling within typical global ranges. From a performance perspective, CaO and MgO, particularly in their free forms (f-CaO and f-MgO), play a critical role in volume stability, as their hydration can induce delayed expansion and potential cracking in concrete. The elevated MgO content may further contribute to long-term expansion risks. In contrast, SiO<sub>2</sub> contributes to structural stability, while Fe<sub>2</sub>O<sub>3</sub> influences density and thermal behaviour but has a limited contribution to cementitious reactivity. These characteristics highlight the importance of controlling f-CaO and f-MgO contents to ensure the durability and dimensional stability of SS-based concrete.

**Table 2.** Basic chemical composition (%) of Formosa SS

Type of SS	BOF040	BOF 010	CAST 040	CAST 010	DeS	BOF (*)	LF (*)
CaO	40.07	37.33	36.97	33.37	46.07	39.4–52.266	40.19–56.7
SiO <sub>2</sub>	11.03	11.1	12.33	12.23	12.3	10.8–18.46	12.49–23.0
Fe <sub>2</sub> O <sub>3</sub>	28.8	29.13	26.4	31.33	16.03	15.57–32.0	1.47–2.38
MgO	7.35	6.75	6.06	6.86	2.82	2.746–9.69	6.7–19.38
Al <sub>2</sub> O <sub>3</sub>	2.8	3.36	5.09	6.69	1.84	1.9–4.59	1.3–9.36
MnO	1.33	1.5	1.8	2.12	0.31	0.828–5.20	0.2–0.936
SO <sub>3</sub>	0.05	0.06	0.15	0.04	1.73	0.12–0.749	0.548–1.63
TiO <sub>2</sub>	0.28	0.3	0.33	0.36	0.18	0.4–2.44	0.3–2.04
K <sub>2</sub> O	0.053	0.047	0.05	0.054	0.047	0.05–0.42	0.01–0.3
Na <sub>2</sub> O	0.39	0.26	0.11	0.09	0.07	–	–
Cl <sup>-</sup>	0.015	0.013	0.013	0.021	0.029	–	–
P <sub>2</sub> O <sub>5</sub>	2.24	1.97	–	–	–	1–2.205	0.0179–0.03
f-CaO	0.56	0.52	0.43	0.36	0.14	–	–

*Note of Table 2:* (\*) Chemical composition data for BOF slag (in UK, France, India, Iran, and the USA) and LF slag (in Spain, Greece, and Italy) provided by Liu et al. [6]. “–” means ‘Not available data’. The decimal values are retained as in the original data.

### 3.3 Grading

The particle size distribution of the used Formosa SS was determined in accordance with TCVN 7572:2006 [47], and the obtained results are shown in Fig. 3. In this figure, the dashed and solid lines

are the grading envelopes for fine and coarse concrete aggregates, with a nominal maximum size  $D_{\max} \leq 40$  mm, as specified by TCVN 7570:2006 [48] and ASTM C33/C33M-18 [49], respectively.

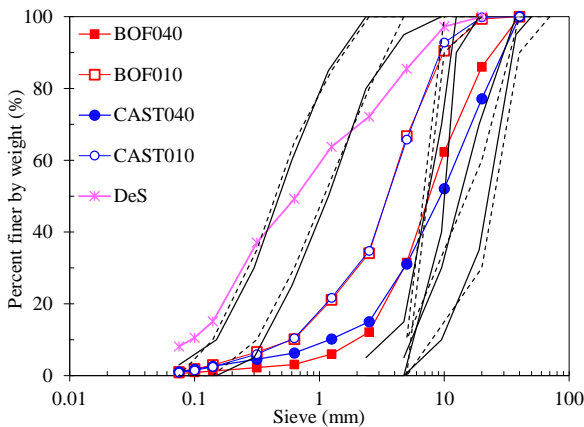


**Fig. 3.** Particle size distribution curves of Formosa SS. The dashed and solid black lines represent the grading envelopes for fine and coarse aggregates according to TCVN 7570:2006 (nominal sizes of 5–10 mm and 5–40 mm) and ASTM C33/C33M-18 (size ranges of 4.75–12.5 mm and 4.75–37.5 mm), respectively.

The grain size of Formosa SS depends on the on-site treatment and recovery processes at the steel plant. As shown in Figs. 2 and 3, significant size variability exists among the different products of the same SS type (e.g., BOF040 versus BOF010 and CAST040 versus CAST010) while SS within the same size category (i.e., 0–10 mm and 0–40 mm) exhibits comparable grading characteristics. In addition, these SSs are recovered with a  $D_{max}$  of 40 mm and 10 mm, and they consist of a wide range of particle sizes and do not comply with the requirements for either fine or coarse aggregates as defined by TCVN 7570:2006 and ASTM C33/C33M-18 (Fig. 3). The results in Fig. 3 also indicate that DeS slag is characterised by a significantly high content of fine aggregate (over 85% of particles finer than 5 mm), and therefore its grading is different from those of other Formosa SSs.

Based on the results in Fig. 3, and to facilitate recycling in concrete applications, we classified the mass percentage of Formosa SS into fine and coarse aggregate fractions in accordance with TCVN 7570:2006, as summarised in Table 3. BOF040 and CAST040 slags ( $D_{max} = 40$  mm) contain approximately 69.4–71.1% coarse

aggregate and 26.6–29.3% fine aggregate, indicating a grading suitable for use as coarse aggregate in concrete. In contrast, BOF010 and CAST010 slags ( $D_{max} = 10$  mm) are dominated by fine particles, accounting for 63.3–63.8%, with only 33.3–34.2% coarse fraction, suggesting their more appropriate use as fine aggregate or blended material.

The proportion of particles finer than 0.14 mm in these SSs ranges from 1.6 to 2.9%, satisfying the limits specified in TCVN 7570:2006 for concrete aggregates. Conversely, DeS slag exhibits an unfavourable grading, with only 14.5% coarse aggregate, 70.4% fine aggregate, and more than 15% of particles finer than 0.14 mm. Such an excessively fine and less coarse aggregate renders it unsuitable for direct use as concrete aggregate. Overall, after classification, BOF040 and CAST040 slags meet the grading requirements for coarse aggregate in concrete, while BOF010 and CAST010 slags may be considered for fine aggregate applications. DeS slag, however, is unsuitable for use in this study and was, therefore, excluded from subsequent experimental phases.

**Table 3.** Grain content (%) of Formosa SS relative to aggregate size classifications according to TCVN 7570:2006

SS type	< 0.14 mm (*)	Fine aggregate		Coarse aggregate		
		0.14–5 mm	5–10 mm	10–20 mm	20–40 mm	40–70 mm
BOF040	1.2	29.3	29.8	23.0	13.5	3.1
BOF010	2.9	63.8	23.8	8.9	0.6	0.0
CAST040	2.4	26.6	19.5	23.0	21.0	7.6
CAST010	2.4	63.3	27.0	7.1	0.1	0.0
DeS	15.1	70.4	11.8	2.7	0.0	0.0

*Note of Table 3:* (\*) According to TCVN 7570:2006 and TCVN 9205:2012 [50] standards, the content of particles finer than 0.14 mm in fine aggregate for concrete must be less than 10% and 15%, respectively.

### 3.4 Physico-mechanical properties

In this section, four types of Formosa SS, namely BOF040, BOF010, CAST040, and CAST010 (hereafter referred to as BOF and CAST slags), were tested to determine their physico-mechanical properties in accordance with the TCVN 7572:2006 standard series. This is to evaluate their compliance with current technical regulations,

including TCVN 7570:2006, TCVN 9205:2012 and TCVN 11969:2018 [51]. Prior to testing, oversized particles (>40 mm) were removed to align with the designated recovery ( $D_{max} = 40$  mm) and to satisfy particle size classification requirements of the aforementioned standards. The experimental results are summarised in Table 4.

**Table 4.** Properties of BOF and CAST slags used as aggregates for concrete

Type of SS	Particle size (mm)	BOF 040	BOF 010	CAST 040	CAST 010
Apparent specific gravity ( $\rho_a$ , g/cm <sup>3</sup> )	0.14–5	3.52	3.59	3.43	3.50
	5–40	3.54	3.47	3.43	3.51
Oven-dry bulk density ( $\rho_k$ , g/cm <sup>3</sup> )	0.14–5	3.11	3.13	2.98	3.07
	5–40	3.33	3.26	3.24	3.27
Saturated-surface-dry bulk density ( $\rho_{hb}$ , g/cm <sup>3</sup> )	0.14–5	3.22	3.26	3.11	3.19
	5–40	3.39	3.32	3.29	3.34
Water absorption ( $w_a$ , %)	0.14–5	3.75	4.03	4.44	3.95
	5–40	1.76	1.91	1.76	2.03
Loose bulk density ( $\rho_x$ , kg/m <sup>3</sup> )	–	1,958	2,025	2,057	1,918
Porosity ( $v_w$ , %)	–	39.2	36.6	35.6	39.5
Water content ( $w$ , %)	–	2.0	3.1	3.8	3.7
Fines content ( $S_c$ , %) (*)	–	0.5	1.0	1.0	0.9
Dried crushing value ( $N_{dk}$ , %)	5–10	3.97	3.42	4.33	2.92
	10–20	6.91	8.06	6.67	5.75
	20–40	11.96	–	12.35	–
Saturated crushing value ( $N_{ds}$ , %)	5–10	4.25	5.25	4.83	4.00
	10–20	9.33	9.31	8.25	8.08
	20–40	13.20	–	15.16	–
Softening coefficient ( $K_M$ )	5–10	0.93	0.65	0.90	0.73
	10–20	0.74	0.87	0.81	0.71
	20–40	0.91	–	0.81	–
Los Angeles abrasion value ( $H_m$ , %)	A	16.45	–	20.16	–
	B	16.25	19.32	17.17	18.37
	C	12.47	13.51	13.97	14.20
	D	13.45	15.28	12.99	14.57
Elongation and flakiness index ( $T_d$ , %)	5–10	4.0	3.6	3.6	3.3
	10–20	1.3	1.4	1.4	2.0
	20–40	2.4	–	2.1	–

*Note of Table 4:* (\*) According to TCVN 11969:2018, the content of particles finer than 0.075 mm in Type I recycled coarse aggregate for concrete must be less than 2%. According to TCVN 9205:2012, this limit for crushed sand is 16% for general concrete, and 9% for structures subjected to abrasion and impact. Per ASTM C33/C33M-18, the allowable fines content (<0.075 mm) for concrete aggregates in non-abrasive applications is ≤5%; for recycled aggregates, the limits are ≤5% and ≤7% for abrasive and non-abrasive concrete applications, respectively. “–” means ‘Not applicable’.

It can be observed that with a chemical composition predominantly consisting of metal oxides, particularly CaO, SiO<sub>2</sub>, Fe<sub>2</sub>O<sub>3</sub>, and MgO accounting for more than 80%, the apparent specific gravity ( $\rho_a$ ) of the BOF and CAST slags is approximately 3.5 g/cm<sup>3</sup> (ranging from 3.43 to 3.59 g/cm<sup>3</sup>). The oven-dry and saturated-surface-dry bulk densities generally exceed 3.0 g/cm<sup>3</sup>, with values of  $\rho_k$  being 2.98–3.33 g/cm<sup>3</sup> and  $\rho_{hb}$  being 3.11–3.39 g/cm<sup>3</sup>, respectively. The loose bulk density ( $\rho_x$ ) is around 2.0 t/m<sup>3</sup> (1,918–2,057 kg/m<sup>3</sup>). These density parameters appear largely independent of the slag type or particle size and are significantly higher than those of natural aggregates. These results satisfy the requirements for Type I recycled coarse aggregates, according to TCVN 11969:2018. Because of their rough and angular surface texture with open pores, the BOF and CAST slags show higher water absorption and moisture content compared with natural aggregates, particularly for the case of fine aggregates. Comparing the results in Table 4 with the specifications of TCVN 11969:2018 and TCVN 9205:2012 confirms that the tested SSS satisfy the requirements for Type I recycled coarse aggregate and fine aggregate used in concrete structures subjected to abrasion and impact. Regarding the silt, dust and clay content according to TCVN 7570:2006, the BOF and CAST slags meet the criteria for coarse aggregate in concrete with grades higher than M400. The saturated crushing values ( $N_{ds}$ ) increase with grain size, approximately 4–5%, 8–9% and 13–15% for 5–10 mm, 10–20 mm, and 20–40 mm fractions, respectively. These results demonstrate the excellent hardness and impact resistance of the used SSS, satisfying the requirements for crushed stone strength grades 120–140 under TCVN 7570:2006, as well as for Type I recycled coarse aggregate under TCVN 11969:2018.

The Los Angeles abrasion loss ( $H_m$ ) of the BOF and CAST slags across all grading classes (A,

B, C, and D) ranges from 12.5 to 20.2%. These values clearly satisfy the criteria of  $H_m \leq 50\%$  for concrete aggregate as specified in TCVN 7570:2006 and TCVN 11969:2018. Because of the rapid cooling from a molten state, followed by controlled crushing and screening, particles of the BOF and CAST slags exhibit a relatively uniform morphology (as shown in Fig. 2). Consequently, the elongation and flakiness index remains in the range from 1.3 to 4.0%, complying with the requirements for aggregate in concrete grades exceeding M400 ( $\leq 15\%$ ) and for Type I recycled coarse aggregate for concrete ( $\leq 35\%$ ).

## 4 Mixtures of Formosa SS for use as concrete aggregates

### 4.1 Types of Formosa SS Mixture

For optimising the recycling and utilisation of SS, a representative mixture of BOF and CAST slags was first established based on their actual generation ratios at the FHS plant (BOF040: 73.7%, BOF010: 18.4%, CAST040: 6.3%, and CAST010: 1.6%).

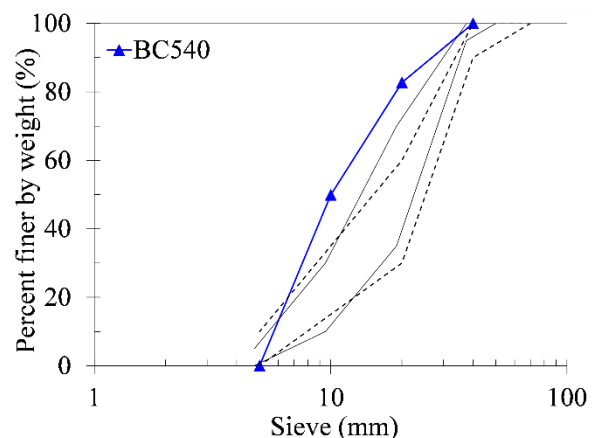


Fig. 4. Particle size distribution of BC540 compared with grading limits of TCVN 7570:2006 (5–40 mm, dashed lines) and ASTM C33/C33M-18 (4.75–37.5 mm, solid lines)



**Fig. 5.** Photos of crushed stone and Ha Tinh sand samples

This initial proportion ensures that the material used in this study reflects real production conditions. For meeting the grading requirements for concrete aggregates, the combined slag was subsequently sieved into standard size ranges, thereby maintaining representativeness while ensuring compliance with TCVN 7570:2006. Four gradations were obtained, namely 5–10 mm, 5–20 mm, 10–40 mm, and 5–40 mm, and were designated as BC510, BC520, BC1040, and BC540, respectively (where “B” and “C” denote BOF and CAST slags, and the numbers indicate particle size ranges). Among these gradations, BC510, BC520, and BC540 generally correspond to the aggregate size ranges specified in ASTM C33/C33M-18. The BC1040 mixture shows a slightly finer tendency than the standard envelope but remains within acceptable limits for coarse aggregate use. The BC540 mixture, however, exhibits a pronounced deviation from the prescribed grading curves (Fig. 4), characterised by an unbalanced particle size distribution with insufficient intermediate fractions. This grading condition may adversely affect packing density, workability, and mechanical performance of concrete. Therefore, BC540 was excluded from subsequent analyses.

For comparison, conventional crushed stone with corresponding size ranges (5–10 mm, 5–20 mm, and 10–40 mm) was used and designated as CS510, CS520, and CS1040. A coarse river sand currently used in Ha Tinh Province was adopted as fine aggregate for all mixtures (hereafter referred to as Ha Tinh sand). Typical photos of the crushed stone and Ha Tinh sand are shown in Fig. 5.

#### 4.2 Properties of the aggregates used for concrete

The grain size distribution curves of Ha Tinh sand, SS mixtures (BC510, BC520, and BC1040), and crushed stones (CS510, CS520, and CS1040) are presented in Figs. 6a–b together with the grading envelopes specified in TCVN 7570:2006 and ASTM C33/C33M-18. The results indicate that all natural aggregates fully satisfy the grading requirements. For SS mixtures, BC510 conforms well to the specified limits as a single-sized aggregate; BC520 lies close to the lower boundary, and BC1040 exhibits a slightly finer distribution. Nevertheless, all SS mixtures remain within the acceptable limits defined by current standards, thereby ensuring consistency with the observations in Section 4.1.

The physical and mechanical properties of the aggregates are summarised in Tables 5 and 6. The apparent specific gravity and bulk density (oven-dry and saturated) of SS mixtures are approximately 1.23–1.28 times higher than those of crushed stone, while their loose bulk density is 1.28–1.42 times higher. Consequently, SS mixtures exhibit slightly lower porosity (44–48%) than crushed stone (50–51%), which is advantageous for concrete mix designs. In addition, the SS mixtures demonstrate superior mechanical performance, with significantly lower crushing values and Los Angeles abrasion losses. Their flakiness index (1.7–2.8%) is well below the limits

specified for high-strength concrete ( $\leq 15\%$ ) and recycled aggregates ( $\leq 35\%$ ), according to TCVN 7570:2006 and TCVN 11969:2018.

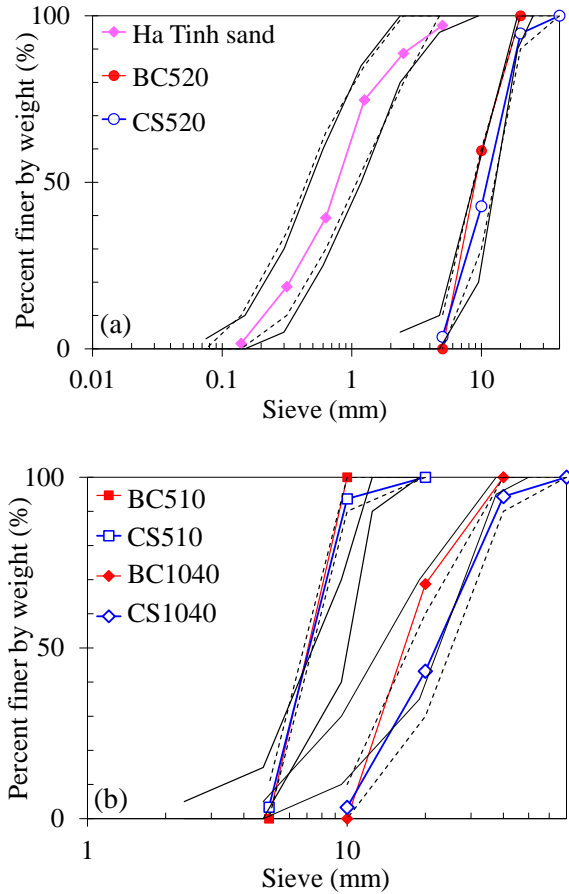


**Fig. 6.** Particle size distributions of Ha Tinh sand, SS mixtures, and crushed stones compared with grading limits of TCVN 7570:2006 (dashed lines) and ASTM C33/C33M-18 (solid lines): (a) fine aggregate and 5–20 mm (4.75–19.0 mm ASTM); (b) 5–10 mm and 10–40 mm (4.75–12.5 mm and 4.75–37.5 mm ASTM)

Generally, despite minor variations in grading characteristics, the experimental results confirm that BOF and CAST slags, as well as their mixtures (BC510, BC520, and BC1040), satisfy the requirements for use as coarse aggregates in M400 concrete. Accordingly, these three SS mixtures were selected for subsequent concrete production and testing, together with Ha Tinh sand as fine aggregate. Reference concrete mixtures with crushed stone (CS510, CS520, and CS1040) were also prepared for comparison.

**Table 5.** Properties of SS mixtures used as aggregates for concrete

Properties	BC510	BC520	BC1040
$\rho_a$ , g/cm <sup>3</sup>	3.51	3.51	3.47
$\rho_k$ , g/cm <sup>3</sup>	3.32	3.34	3.34
$\rho_{bh}$ , g/cm <sup>3</sup>	3.37	3.38	3.38
$w_a$ , %	1.68	1.47	1.13
$\rho_x$ , kg/m <sup>3</sup>	1724	1878	1872
$v_w$ , %	48.1	43.7	44.0
$S_c$ , % (*)	0.0	0.0	0.0
$N_{dk}$ , %	2.88	5.18	8.76
$N_{ds}$ , %	3.25	6.44	10.72
$K_M$	0.88	0.80	0.82
$H_m$ , %	10.2	14.34	15.85
$T_d$ , %	2.8	2.8	1.7

**Table 6.** Properties of Ha Tinh sand and crushed stones used as aggregates for concrete

Properties	CS510	CS520	CS1040	Ha Tinh sand
$\rho_a$ , g/cm <sup>3</sup>	2.75	2.74	2.72	2.69
$\rho_k$ , g/cm <sup>3</sup>	2.69	2.71	2.70	2.45
$\rho_{bh}$ , g/cm <sup>3</sup>	2.71	2.72	2.71	2.54
$w_a$ , %	0.76	0.50	0.39	3.68
$\rho_x$ , kg/m <sup>3</sup>	1346	1327	1342	1436
$v_w$ , %	50.0	51.0	50.2	41.4
$S_c$ , % (*)	0.7	0.5	0.6	0.8/0.0 (**)
$N_{dk}$ , %	7.38	6.63	9.37	–
$N_{ds}$ , %	8.63	9.50	10.11	–
$K_M$	0.86	0.70	0.93	–
$H_m$ , %	21.60	18.06	16.74	–
$T_d$ , %	–	–	–	–

Note of Tables 5 and 6: (\*) For SS mixtures, this value refers to the content of particles finer than 0.075 mm; for the crushed stones and Ha Tinh sand, it represents the contents of dust, silt, and clay in the aggregate, as well as the clay lump content in the fine aggregate. (\*\*) For Ha Tinh sand, 0.8% denotes the total dust, silt, and clay content, while 0.0% indicates the content of clay lumps. “–” means ‘Not applicable’ or ‘no data’.

## 5 Concrete incorporating Formosa SS mixtures as coarse aggregates

### 5.1 Concrete mixtures

Based on the results in Tables 5 and 6, we developed concrete mix proportions for both SS and CS concretes. Owing to their higher density, SS mixtures are particularly suitable for heavyweight concrete applications, such as wave-dissipating units (e.g., Tetrapod blocks). Accordingly, all mixtures were designed to achieve M400 compressive strength, with a target slump of 6–8 cm and enhanced sulfate resistance. The concrete mix design was carried out by using the absolute volume method to determine the quantities of cement, water, and aggregates per cubic meter. However, conventional mix design approaches are primarily established for natural aggregates and do not fully account for the distinct characteristics of SS, including higher density, angularity, rough surface texture, and water absorption. Therefore, the mix proportions were initially determined according to the technical guidelines of the Ministry of Construction (Dispatch No. 1784/BXD-VP) [52], and subsequently refined through trial batches to ensure both performance and workability. The specified mix proportions for M400 concrete with a target slump of 6–8 cm, corresponding to each coarse aggregate size (5–10 mm, 5–20 mm and 10–40 mm), are presented in Table 7.

In Table 7, the quantity of cement and water is specified directly with mass (cement, kg) and volume (water, L), whereas aggregates are provided with volume (m<sup>3</sup>). Therefore, the aggregate volumes were converted to mass from the obtained results of loose bulk density in Tables 5 and 6. It is noted that this approach may introduce some approximation, as loose bulk density does not fully represent the compacted state of aggregates in concrete; however, it provides a practical and commonly adopted basis

for mix proportioning, especially when combined with experimental validation. PCB 40 cement and tap water from the laboratory were used for all mixtures. Sikacrete PP-1 admixture was used to ensure sulfate resistance, and Sikaplast-361 admixture, a superplasticiser instead of a conventional plasticiser, was employed to enhance the workability of the fresh concrete as suggested by Uemura et al. [46]. The dosages of these admixtures, following the recommendations of the manufacturer, were 5% of the cement mass and 800 mL per 100 kg of cement, respectively. The calculated mix proportions for SS and CS concretes corresponding to each coarse aggregate size are presented in Tables 8 and 9.

**Table 7.** M400 concrete mixtures according to the guidelines of MOC

Mixture	<i>D</i> <sub>max</sub> of coarse aggregate (mm)		
	10	20	40
PCB 40 cement (kg)	483	453	423
Fine aggregate (coarse river sand) (m <sup>3</sup> )	0.402	0.416	0.432
Coarse aggregate (crushed stone) (m <sup>3</sup> )	0.813	0.828	0.840
Water (L)	193	181	169
Admixture	Plasticiser		

**Table 8.** Calculated mixture proportions for 1 m<sup>3</sup> of SS concretes

Mixture	BC 510	BC 520	BC 1040
PCB 40 cement (kg)	483	453	423
Ha Tinh sand (kg)	577.4	597.5	620.5
SS mixture or crushed stone (kg)	1,401.3	1,555.0	1,572.5
Water (L)	193	181	169
Sikacrete PP-1 admixture (kg)	24.2	22.7	21.2
Sikaplast-316 admixture (mL)	3,864	3,624	3,384

**Table 9.** Calculated mixture proportions for 1 m<sup>3</sup> of CS concretes

Mixture	CS 510	CS 520	CS 1040
PCB 40 cement (kg)	483	453	423
Ha Tinh sand (kg)	577.4	597.5	620.5
SS mixture or crushed stone (kg)	1,094.2	1,098.5	1,127.0
Water (L)	193	181	169
Sikacrete PP-1 admixture (kg)	24.2	22.7	21.2
Sikaplast-316 admixture (mL)	3864	3,624	3,384

## 5.2 Concrete properties

The fresh concrete mixtures were prepared with a free-fall mixer, and the slump tests were carried out in accordance with TCVN 3106:2022 [53]. 150 mm cubic concrete specimens were cast and water-cured following TCVN 3105:2022 [54] prior to compression testing. The concrete mixture proportions in Tables 8 and 9 were determined following the guidelines for natural coarse aggregate (crushed stone). However, since the SS mixtures exhibit lower porosity than the crushed stone (as previously presented in Tables 5 and 6), adjustments to the calculation in Tables 8 and 9 were required. The practical casting results indicated that the material quantities for the SS concretes had to be increased with the factors of 1.10, 1.13, and 1.12 for BC510, BC520, and BC1040, respectively, to achieve the target concrete volume. These factors were introduced to account for the higher density and different packing behaviours of SS compared with natural aggregates, as well as to compensate for potential differences in void structure and workability observed during preliminary trials. For the CS concretes, the mix proportions for CS510 concrete remained unchanged, while those for the CS520 and CS1040 concretes required an increase with the factors of 1.06 and 1.05, respectively.

Accordingly, the final adjusted mix proportions for 1 m<sup>3</sup> of SS and CS concretes, based on the actual casting results, are summarised in Tables 10 and 11.

**Table 10.** Calculated mixture proportions for 1 m<sup>3</sup> of SS concretes after adjustment

Mixture	BC 510	BC 520	BC 1040
PCB 40 cement (kg)	531.3	511.9	473.8
Ha Tinh sand (kg)	635.1	675.2	695.0
SS mixture or crushed stone (kg)	1,541.4	1,757.2	1,761.2
Water (L)	212.3	204.5	189.3
Sikacrete PP-1 admixture (kg)	26.6	25.7	23.7
Sikaplast-316 admixture (mL)	4,250.4	4,095.1	3,790.1

**Table 11.** Calculated mixture proportions for 1 m<sup>3</sup> of CS concretes after adjustment

Mixture	CS 510	CS 520	CS 1040
PCB 40 cement (kg)	483.0	480.2	444.2
Ha Tinh sand (kg)	577.4	633.4	651.5
SS mixture or crushed stone (kg)	1,094.2	1,164.4	1,183.4
Water (L)	193.0	191.9	177.5
Sikacrete PP-1 admixture (kg)	24.2	24.1	22.3
Sikaplast-316 admixture (mL)	3,864.0	3841.4	3,553.2

With the use of a superplasticiser at a  $w/c$  ratio of 0.4, the slump of the SS concretes reached 6.5–8.5 cm, whereas the CS concretes exhibited a wider range of 6.0–13.5 cm. For each concrete type, a set of three specimens was tested in accordance with TCVN 3118:2022 [55] to determine the compressive strength at the ages of 3, 7, and 28 days. The deformation of the specimens was also measured to determine the strain during testing. The photos of the concrete

specimens after the compression test, showing the situation of SS mixtures and crushed stones incorporated as coarse aggregates, are presented in Figs. 7 and 8, respectively.



**Fig. 7.** Photos of SS concrete specimens after compression test: (a) BC510; (b) BC520; (c) BC1040. For each concrete type, specimens from bottom to top correspond to water-cured ages of 3, 7, and 28 days

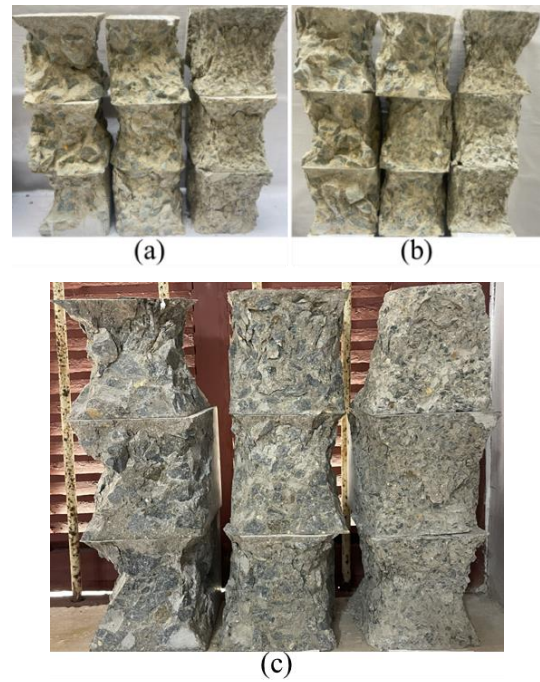


**Fig. 8.** Photos of CS concrete specimens after compression test at water-cured ages of (a) 3 days; (b) 7 days; (c) 28 days. For each curing age, the specimens from left to right correspond to CS1040, CS520 and CS510 concrete.

### Compressive stress-strain relationship

The compressive stress-strain relationships of all SS and CS concrete specimens, resulting from the recorded compressive stress ( $R$ , MPa) and deformation ( $d$ , mm) during testing, are presented in Figs. 9 and 10, respectively. In the initial loading stage, the compressive stress increases with strain ( $\epsilon$ , mm/mm), reaching a peak value corresponding to the compressive strength of concrete ( $R_N$ , MPa), and then decreases with the strain when failure occurs. The strain corresponding to  $R_N$  is defined as the strain at failure ( $\epsilon_{phN}$ , mm/mm). With the exception of the relatively scattered results for BC510 concrete (Fig. 9a), the values of  $\epsilon_{phN}$  for BC520 and BC1040 concrete specimens exhibit greater consistency than those of the CS concrete specimens, particularly after 7 days of curing, when the concrete has attained a significant strength.

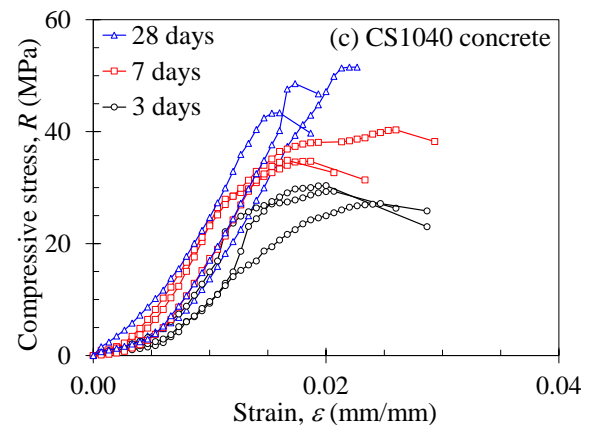
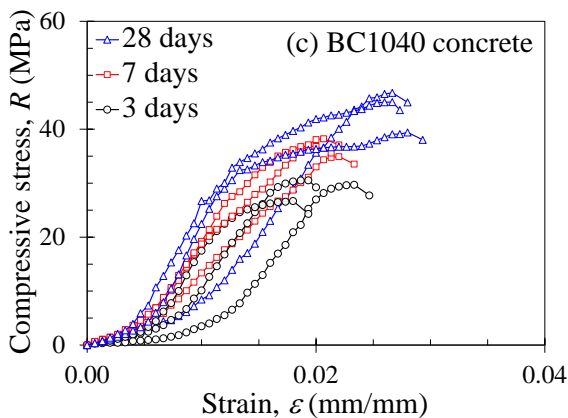
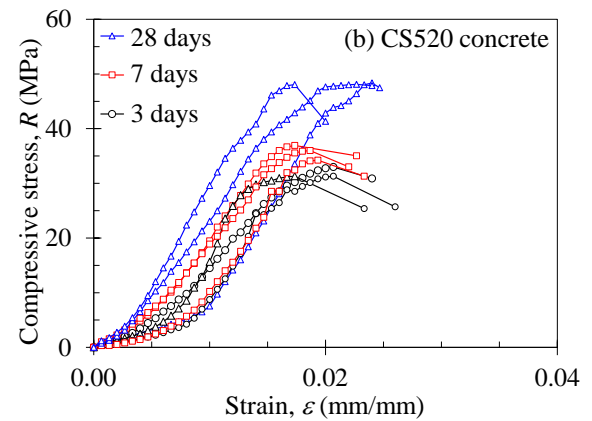
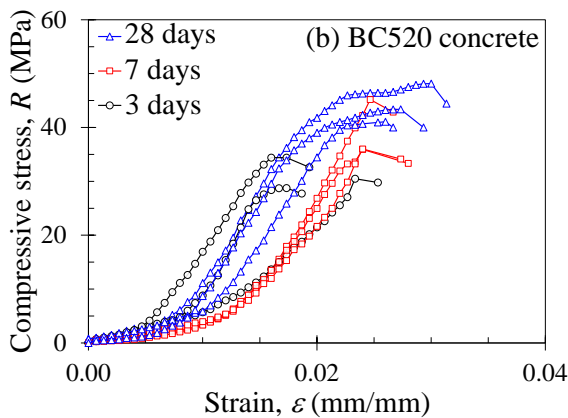
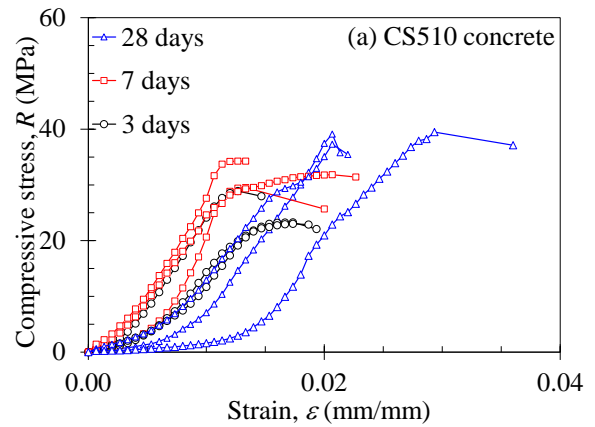
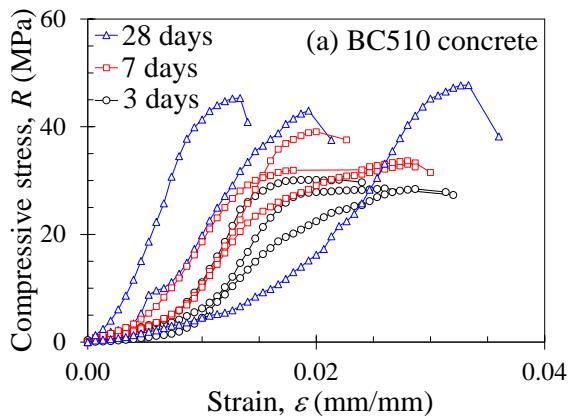


Fig. 9. Compressive stress-strain relationships of SS concretes

Fig. 10. Compressive stress-strain relationships of CS concretes

In Fig. 11, the experimental values of  $\epsilon_{phN}$  are plotted against the curing duration ( $t$ , days) with symbols, while the average values are shown with dashed and solid lines. It has been reported that, owing to the rough surface texture with the presence of open pores, SS aggregates exhibit better interlocking and bonding with the cement

matrix [6, 11], which may result in a greater strain at failure than that of conventional concrete. Because of the relatively large scatter of the  $\varepsilon_{phN}$  values for BC510 concrete at 28 days, a decreasing tendency of  $\varepsilon_{phN}$  with  $t$  is observed with this concrete. In contrast, BC520 and BC1040 concretes exhibit an opposite trend, i.e.  $\varepsilon_{phN}$  increases with  $t$ , and the results of the specimens test show good consistency. When  $t = 28$  days, the strain at failure of BC520 and BC1040 concretes reaches approximately 0.025–0.030 mm/mm, which is higher than the values of 0.015–0.025 mm/mm obtained with CS concretes. It should be noted that these strain values are relatively high compared with typical ranges reported for conventional concrete. This may be attributed to the differences in the strain measurement method, including instrumentation type, gauge length, and data processing approach, which can significantly influence the recorded values. Therefore, further clarification and standardisation of the measurement procedure are necessary to ensure comparability and reliability of the results.

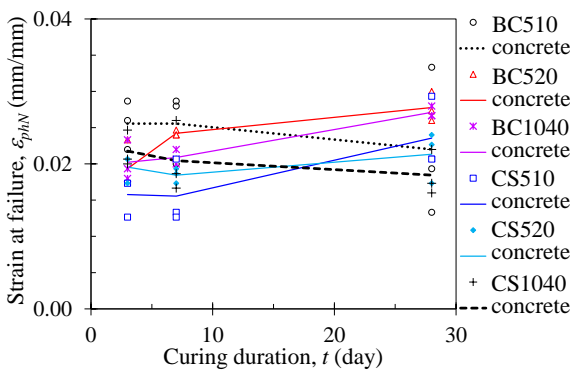


Fig. 11. Strain at failure of SS and CS concretes

### Compressive strength

Fig. 12 illustrates and compares the compressive strength development with curing time and between the concrete types; the experimental and average values of  $R_N$  (MPa) are shown against  $t$  with similar symbols, solid and dashed lines to the those in Fig. 11. The expected compressive

strength of M400 concrete at 3, 7, and 28 days (denoted as  $R_{N3}$ ,  $R_{N7}$ , and  $R_{N28}$ ), based on empirical data, are also included for reference. A comparison between the average values of  $R_{N28}$  and the cement content (as shown in Table 8) reveals that, for the SS concretes,  $R_{N28}$  increases with the cement content. Compared with M400 concrete relative to the required values of  $R_{N28}$ , the BC510, BC520, and BC1040 concretes achieve 117.8, 114.8, and 113.6%, respectively. For the CS concretes, despite using the lowest cement content, the CS1040 concrete exhibits a comparable value of  $R_{N28}$  to that of CS520 concrete, which has a higher cement content, corresponding to 124.2 and 125.1% of the required M400 strength. In contrast, although having the highest cement content, the CS510 concrete shows the lowest compressive strength development, which is equal to the M400's requirement at 28 days. In addition, the results in Fig. 12 also indicate that the compressive strength development of SS concretes is more consistent than that of the CS concretes.

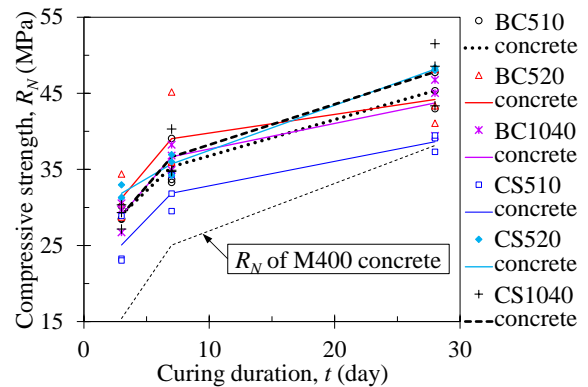


Fig. 12. Compressive strength development with curing duration of SS and CS concretes

### Concrete density

In order to compare and evaluate the density of the SS and CS concretes, we present the photos of SS concrete specimens before compression testing in Fig. 13 and their density development ( $\rho_c$ , t/m<sup>3</sup>) against  $t$  in Fig. 14. The experimental and average

values are shown with the same symbols, solid and dashed lines as those in Figs. 11 and 12.

The conventional concretes used in this study (CS510, CS520, and CS1040) exhibit density values of 2.33, 2.36, and 2.37 t/m<sup>3</sup>, respectively (Fig. 14). In contrast, the average masses of the 150 mm cubic specimens for BC510, BC520, and BC1040 concretes are 8.921, 9.228, and 9.176 kg (Fig. 13), corresponding to densities of 2.64, 2.73, and 2.72 t/m<sup>3</sup>. Accordingly, the SS concretes incorporating Formosa SS as coarse aggregate show densities approximately 1.13–1.16 times higher than those of conventional concretes. This increase is a key characteristic of heavyweight concrete and is particularly relevant for applications where higher self-weight is beneficial, such as gravity-based or impact-resistant structures. In the context of coastal engineering, higher-density concrete may contribute to improved stability of structural units under wave action, as confirmed in the previous studies [46, 56]. However, it should be emphasised that no direct assessment of wave-dissipation performance was conducted in this study; therefore, such benefits can only be considered as potential. Among the SS concretes, BC520 and BC1040 exhibit slightly higher densities than BC510 because of their broader gradation and higher SS content, offering increased SS utilisation and suitability for higher-density concrete applications.

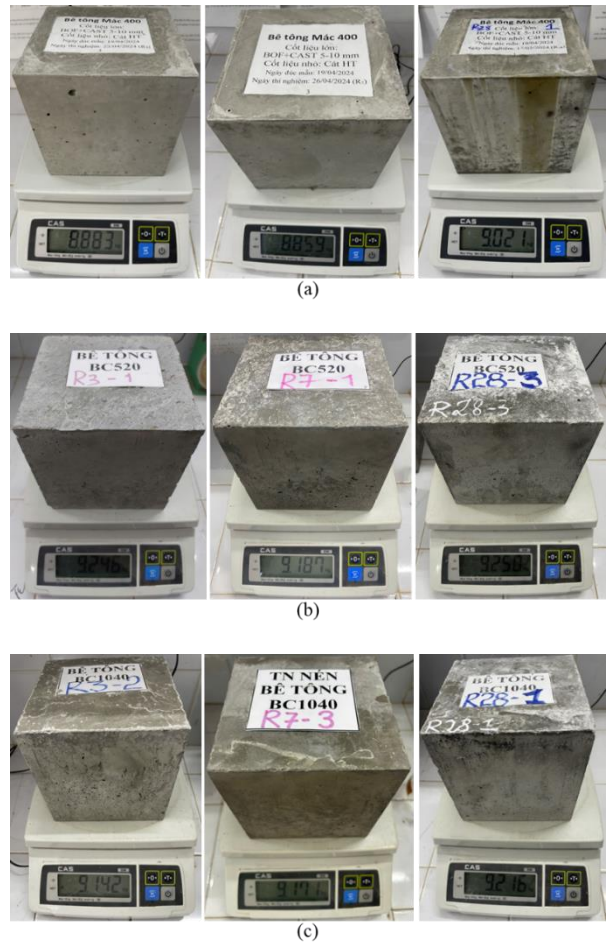


Fig. 13. Typical photos of 150 mm cubic specimens of SS concretes: (a) BC510; (b) BC520; (c) BC1040

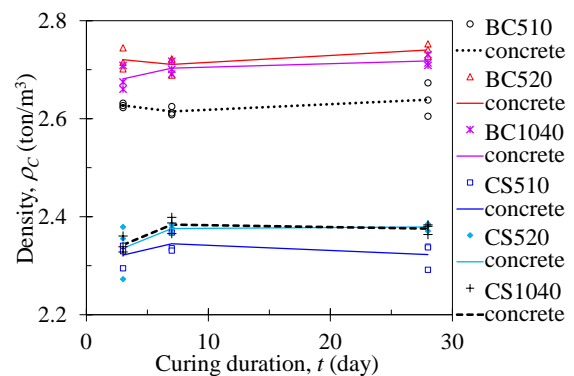


Fig. 14. Density of SS and CS concretes with curing duration

## 6 Conclusions

This study demonstrates that, because of their similar chemical composition, physico-mechanical properties, and particle size fractions, BOF and

CAST slags can be combined according to actual production ratios for use as coarse aggregates in concrete, contributing to more efficient recycling of SS. The obtained results facilitated the main conclusions, as follows:

Although SS in Vietnam is typically recovered in the size ranges unsuitable for direct use in concrete, the BOF and CAST slags investigated in this study satisfy current standards for aggregates in M400 concrete and for Type I recycled coarse aggregates.

The proposed SS mixtures (5–10 mm, 5–20 mm, and 10–40 mm) generally comply with grading requirements and exhibit superior mechanical properties compared with natural crushed stone with similar gradation.

Concretes incorporating SS aggregates show stable strength development and higher strain at failure. The 28-day compressive strength reaches 113.6–117.8% of the target M400 strength. However, the comparison between SS and conventional concretes is influenced by mix design adjustments and therefore should be interpreted with caution.

Because of the high density of SS aggregates, the resulting concretes achieve densities of 2.64–2.73 t/m<sup>3</sup>, approximately 1.13–1.16 times higher than those of conventional concretes, meeting the requirements for heavyweight concrete.

The higher density and satisfactory mechanical performance indicate the potential suitability of SS concrete for applications requiring heavyweight materials, such as wave-dissipating structures; however, this has not been directly validated in this study. Therefore, further research should focus on long-term durability, marine exposure conditions, and structural-scale or hydraulic performance to validate the practical application of SS concrete.

## Acknowledgement

This research was financially supported by the National Foundation for Science and Technology Development – NAFOSTED – under the grant No. NCUD.06-2025.02, and also by Hue University under the Core Research Program, grant No. NCTB.DHH.2025.01. The authors would like to express their sincere gratitude for this support.

## References

1. U.S. Geological Survey (USGS). Mineral commodity summaries 2024. Report. Reston: USGS; 2024. Report No.: 2024.
2. Wang G, Wang Y, Gao Z. Use of steel slag as a granular material: volume expansion prediction and usability criteria. *J Hazard Mater.* 2010; 184:555-60.
3. Wang GC. The utilization of slags in civil infrastructure construction. Woodhead Publishing Series in Civil and Structural Engineering No. 68. UK: Woodhead Publishing; 2016.
4. Grubeša IN, Barišić I, Fucic A, Bansode SS. Characteristics and uses of steel slag in building construction. Woodhead Publishing Series in Civil and Structural Engineering No. 67. UK: Woodhead Publishing; 2016.
5. Guo J, Bao Y, Wang M. Steel slag in China: Treatment, recycling, and management. *Waste Manag.* 2018; 78:318-30.
6. Liu J, Xu J, Liu Q, Wang S, Yu B. Steel slag for roadway construction: A review of material characteristics and application mechanisms. *J Mater Civ Eng.* 2022; 34(6):03122001.
7. News from India PSU. NITI Aayog and Ministry of Steel making efforts to make steel slag production and utilization part of circular economy [Internet]. 2021 [cited 2021 Dec 28]. Available from: <https://indianpsu.com/niti-aayog-and-ministry-of-steel-making-efforts-to-make-steel-slag-production-and-utilization-part-of-circular-economy/>
8. Yildirim IZ, Prezzi M. Geotechnical properties of fresh and aged basic oxygen furnace steel slag. *Journal of Materials in Civil Engineerin.* 2015;27(12):04015046.

9. Wang G. Determination of the expansion force of coarse steel slag aggregate. *Construction and Building Materials*. 2010;24(10):1961-6.
10. Gao J, Sha A, Wang Z, Tong Z, Liu Z. Utilization of steel slag as aggregate in asphalt mixtures for microwave deicing. *Journal of Cleaner Production*. 2017;152:429-42.
11. Guo Y, Xie J, Zhao J, Zuo K. Utilization of unprocessed steel slag as fine aggregate in normal- and high-strength concrete. *Construction and Building Materials*. 2019;204:41-9.
12. Hasita S, Suddeepong A, Horpibulsuk S, Samingthong W, Arulrajah A, Chinkulkijniwat A. Properties of asphalt concrete using aggregates composed of limestone and steel slag blends. *J Mater Civ Eng*. 2020;32(7).
13. Netinger I, Kesegic I, Guljas I. The effects of high temperatures on the mechanical properties of concrete made with different types of aggregates. *Fire Saf J*. 2011;46:425-30.
14. Papayianni I, Anastasiou E. Production of high-strength concrete using high volume of industrial by-products. *Constr Build Mater*. 2010; 24:1412-7.
15. Brand AS, Roesler JR. Steel furnace slag aggregate expansion and hardened concrete properties. *Cem Concr Compos*. 2015;60:1-9.
16. Jiang Y, Ling TC, Shi C, Pan SY. Characteristics of steel slags and their use in cement and concrete: a review. *Resour Conserv Recycl*. 2018;136:187-97.
17. Skaf M, Manso JM, Aragón Á, Fuente-Alonso JA, Ortega-López V. EAF slag in asphalt mixes: A brief review of its possible re-use. *Resour Conserv Recycl*. 2017;120:176-85.
18. Pathak S, Choudhary R, Kumar A, Shukla SK. Evaluation of benefits of open-graded friction courses with basic oxygen furnace steel-slag aggregates for hilly and high-rainfall regions in India. *J Mater Civ Eng*. 2020;32(12):4020356.
19. Yang C, Xie J, Wu S, Amirkhanian S, Wang Z, Song J, et al. Enhancement mechanism of induction heating on blending efficiency of RAP–virgin asphalt in steel slag recycled asphalt mixtures. *Constr Build Mater*. 2021;269:121318.
20. Ameri M, Hesami S, Goli H. Laboratory evaluation of warm mix asphalt mixtures containing electric arc furnace steel slag. *Constr Build Mater*. 2013;49:611-7.
21. Poh HY, Ghataora GS, Ghazireh N. Soil stabilization using basic oxygen steel slag fines. *J Mater Civ Eng*. 2006;18(2):229-40.
22. Shiha M, El-Badawy S, Gabr A. Modeling and performance evaluation of asphalt mixtures and aggregate bases containing steel slag. *Constr Build Mater*. 2020;248:118710.
23. Dang TD, Tuan NM, Phong NT, Tomoo I, Yasutaka T, Ryoichi S. Mechanical properties of steel slag replaced mineral aggregate for road base/sub-base application based on Vietnam and Japan standards. *Environ Sci Pollut Res*. 2021;29:42067-73.
24. World Steel Association. World steel in figures 2025 [Internet]. [cited 2025 Dec 25]. Available from: <https://worldsteel.org/data/world-steel-in-figures/world-steel-in-figures-2025/>.
25. Lam TV. Study on the use of metallurgical slag waste from the Thai Nguyen Iron and Steel Plant as an additive in concrete production for construction works in Thai Nguyen Province [research project]. Thai Nguyen: Thai Nguyen University of Technology; 2010. (In Vietnamese).
26. Lam TV, Hung NX. Study on the utilization of metallurgical waste as aggregates in concrete [report]. VNCOLD; 2015. Available from: <https://vncold.vn/Modules/CMS/Upload/10/KhoaHocCongNghe/150409/PheThaiLuyenKim.pdf>. (In Vietnamese).
27. Gia N, Sua NV. Global utilization of blast furnace slag and steel slag: Environmental protection lessons for the Vietnamese steel industry [Internet]. 2018 [cited 2023 Dec 25]. Available from: <https://tapchimoitruong.vn/>. (In Vietnamese).
28. Hang NTT, Khanh NX, Tieng TV. Discrete element modeling of steel slag concrete. *Lect Notes Netw Syst*. 2018;63:284-90.
29. Hang NTT, Ha MH, Hung PD, Nguyen DL. Responses of concrete using steel slag as coarse aggregate replacement under splitting and flexure. *Sustainability*. 2020;12(12):4913.
30. Nhi TTH, Nhan TT, Quynh TTN, Truong PQ, Huy PV, Dat DP, et al. Evaluation of mechanical properties of Formosa Ha Tinh steel slag as aggregate in concrete. *J Sci Technol Hue Univ*. 2024;24(2):133–44. (In Vietnamese).
31. Phat HT. Investigation of the physico-mechanical properties of Formosa Ha Tinh steel slag for use as coarse aggregate in concrete [MSc thesis]. Hue: University of Sciences – Hue University; 2025. (In Vietnamese).

32. Quoc DT, Nhan TT, Quynh TTN, Thach TX, Hai NT, Thien DQ, et al. Properties of concrete with coarse aggregate using steel slag mixture from Ha Tinh Formosa steel plant. *Hue Univ J Sci Nat Sci.* 2025;134(1C):159-70. (In Vietnamese).
33. Quoc DT, Nhan TT, Quynh TTN, Huyen NTL, Thien DQ, Thach TX, et al. Recycling steel slag as a substitute for natural aggregate in construction. *Hue Univ J Sci Nat Sci.* 2025;134(1S-1):27-41.
34. Le VH, Luong TC, Le VH, Vu VL, Pham VT. Study on the utilization of steel slag as a material for road base construction [report]. Hanoi: Institute of Construction Materials; 2018. (In Vietnamese).
35. Son TH. Study on key properties of fly ash-based geopolymer concrete incorporating steel slag aggregates for highway pavement construction in Vietnam [PhD dissertation]. Hanoi: University of Transport and Communications; 2020. (In Vietnamese).
36. Ha MH. Study on the use of Ba Ria-Vung Tau steel slag in road construction [PhD dissertation]. Hanoi: University of Transport and Communications; 2019. (In Vietnamese).
37. Het NV. Evaluation of the effects of steel slag on the physico-mechanical properties of soil-steel slag mixtures used as road embankment materials [MSc thesis]. Hue: University of Sciences – Hue University; 2025. (In Vietnamese).
38. Luan TV, Song LT, Thien PH. Study on the use of steel slag as filling and embankment materials in construction. *J Mater Constr.* 2021;11(6):68-74.
39. Ministry of Construction. Decision No. 430/QĐ-BXD: Technical guidelines on iron slag and steel slag for use as building materials. Hanoi: Ministry of Construction; 2017. (In Vietnamese).
40. Ministry of Natural Resources and Environment. Circular No. 02/2022/TT-BTNMT. Hanoi: Ministry of Natural Resources and Environment; 2022. (In Vietnamese).
41. Ministry of Science and Technology. TCVN 13906:2024: Steel slag using as backfill material. Hanoi: Ministry of Science and Technology; 2024. (In Vietnamese).
42. Ministry of Science and Technology. TCVN 13908-2:2024: Slag aggregate for concrete – Part 2. Hanoi: Ministry of Science and Technology; 2024. (In Vietnamese).
43. Online map of riverbank and coastal erosion in Vietnam [Internet]. [cited 2025 Dec 10]. Available from: <https://satlo.dmptc.gov.vn/>.
44. Hoi An coastal erosion seen up close as emergency status is declared [Internet]. [cited 2025 Jan 15]. Available from: <https://tienphong.vn/can-canhh-sat-lo-o-bien-hoi-an-khien-phai-cong-bo-tinh-trang-khan-cap-post1707980.tpo>
45. Hudson RY. Laboratory investigation of rubble-mound breakwaters. *J Waterw Harb Div.* 1959;85(3):93-121.
46. Uemura R, Mitsuiishi N, Akahane K, Amma S, Maruyama M, Yamamoto T, et al. Overview of slag usage technology development. *Nippon Steel Tech Rep.* 2015;109:160-82.
47. Ministry of Science and Technology. TCVN 7572:2006: Aggregates for concrete and mortar – Test methods. Hanoi: Ministry of Science and Technology; 2006. (In Vietnamese).
48. Ministry of Science and Technology. TCVN 7570:2006: Aggregates for concrete and mortar – Specifications. Hanoi: Ministry of Science and Technology; 2006. (In Vietnamese).
49. ASTM International. ASTM C33/C33M-18: Standard specification for concrete aggregates; 2018.
50. Ministry of Science and Technology. TCVN 9205:2012: Crushed sand for concrete and mortar. Hanoi: Ministry of Science and Technology; 2012. (In Vietnamese).
51. Ministry of Science and Technology. TCVN 11969:2018: Recycled coarse aggregates for concrete. Hanoi: Ministry of Science and Technology; 2018. (In Vietnamese).
52. Ministry of Construction. Official Dispatch No. 1784/BXD-VP. Hanoi: Ministry of Science and Technology; 2007. (In Vietnamese).
53. Ministry of Science and Technology. TCVN 3106:2022: Fresh concrete – Test method for slump. Hanoi: Ministry of Science and Technology; 2022. (In Vietnamese).
54. Ministry of Science and Technology. TCVN 3105:2022: Concrete – Sampling and curing. Hanoi: Ministry of Science and Technology; 2022. (In Vietnamese).
55. Ministry of Science and Technology. TCVN 3118:2022: Hardened concrete – Compressive

strength test. Hanoi: Ministry of Science and Technology; 2022. (In Vietnamese).

56. Horii K, Tsutsumi N, Kitano Y, Sugahara K. Overview of iron/steel slag application and development. Nippon Steel Tech Rep. 2015;109:5-11.